

for the location of the extra hump, the threshold of the test is changed to maintain the false alarm probability of 0.01. In all cases, if the hump is added in the reference data performance improves, but if the hump is added to the test cell data, performance degrades. This simple example illustrates the use of our equations in an airborne radar application.

We can explain the results in Figs. 1–7 by considering the changes in the pdf of  $\rho$  caused by changes in  $\text{Var}\{d\}$  or  $C$ . In these cases, a decrease in  $\text{Var}\{d\}$  or  $\phi_j$  causes the mass in the pdf of  $\rho$  to move toward larger values of  $\rho$ . Due to the decreasing nature of the function multiplying the pdf of  $\rho$  in the integrand of (30), this causes a decrease in the probability of false alarm. It is possible to apply similar analysis to also explain changes in probability of detection.

## VI. CONCLUSIONS

An analysis of the performance of the adaptive matched filter algorithm has been provided for cases where the data used to estimate the covariance matrix is not matched to the true covariance matrix of the data to be tested. Such cases can occur in nonhomogeneous environments that appear to occur frequently in real radars. Closed-form approximate expressions are given for the probability of false alarm and detection. These expressions apply for any amount of data used in the covariance matrix estimation. The analysis indicates which types of covariance matrix mismatches are important and which types are not. The equations indicate that performance depends on a few critical parameters. An airborne radar example is provided to show that the changes in performance due to mismatch can be significant in some practical situations.

## REFERENCES

- [1] W. S. Chen and I. S. Reed, "A new CFAR detection test for radar," *Digital Signal Process.*, vol. 4, pp. 198–214, Oct. 1991.
- [2] F. Robey, D. Fuhrmann, E. Kelly, and R. Nitzberg, "A CFAR adaptive matched filter detector," *IEEE Trans. Aerosp. Electron. Syst.*, vol. 28, pp. 208–216, Jan. 1992.
- [3] J. S. Goldstein and I. S. Reed, "Theory of partially adaptive radar," *IEEE Trans. Aerosp. Electron. Syst.*, vol. 33, pp. 1309–1325, Oct. 1997.
- [4] R. J. Muirhead, *Aspects of Multivariate Statistical Theory*. New York: Wiley, 1982.
- [5] N. L. Johnson and S. Kotz, *Distributions in Statistics: Continuous Univariate Distributions-2*. Boston, MA: Houghton Mifflin, 1970.
- [6] L. Cai and H. Wang "Further results on adaptive filtering with embedded CFAR," *IEEE Trans. Aerosp. Electron. Syst.*, vol. 30, pp. 1009–1020, Oct. 1994.
- [7] H. Wang and L. Cai, "On adaptive spatial-temporal processing for airborne surveillance radar systems," *IEEE Trans. Aerosp. Electron. Syst.*, vol. 30, pp. 660–669, July 1994.

## Multiresolution ESPRIT Algorithm

Aweke N. Lemma, Alle-Jan van der Veen, and Ed F. Deprettere

**Abstract**—Multiresolution ESPRIT is an extension of the ESPRIT direction finding algorithm to antenna arrays with multiple baselines. A short (half wavelength) baseline is necessary to avoid aliasing, and a long baseline is preferred for accuracy. The MR-ESPRIT algorithm allows the combination of both estimates. The ratio of the longest baseline to the shortest one is a measure of the gain in accuracy. Because of various factors, including noise, signal bandwidth, and measurement error, the achievable gain in accuracy is bounded.

**Index Terms**—Dual shift-invariance, joint diagonalization, multiple baseline, multiresolution ESPRIT.

## I. INTRODUCTION

In many signal processing applications, it is required to estimate signal parameters such as DOA and carrier frequencies from measurement data. To this end, there have been several approaches, including the so-called ESPRIT algorithm [1]. Since its derivation, the ESPRIT algorithm has been used for direction-of-arrival estimation, harmonic analysis, frequency estimation, delay estimation, and combinations thereof. In essence, the algorithm makes use of a single shift invariance structure present in the array response vector  $\mathbf{a}(\theta)$ , where  $\theta = e^{j\mu}$ , and  $\mu$  is a phase shift to be estimated. In narrowband direction-of-arrival estimation, the phase shift is due to the difference in arrival times of the wavefront at the elements of an antenna array. For a uniform linear array (ULA), it is well known that  $\mathbf{a}(\theta) = [1 \ \theta \ \theta^2 \ \dots]^T$  and  $\mu = 2\pi\Delta \sin(\alpha)$ , where  $\Delta$  is the distance between the elements (in wavelengths), and  $\alpha$  is the angle of arrival measured with respect to the normal of the array axis.

It was shown in the literature [2]–[6] that the accuracy of the estimation of  $\sin(\alpha)$  is directly proportional to  $1/\Delta$ . Thus, it is preferable to have a large baseline separation  $\Delta$  so that we collect a large phase shift  $\mu$ . Unfortunately, however, we cannot collect more than a single cycle  $-\pi \leq \mu < \pi$  because the inverse of the mapping  $\mu \rightarrow \theta = e^{j\mu}$  is ambiguous outside this range. To prevent aliasing, we thus have to ensure that  $\Delta \leq 1/2$ , which is essentially Shannon's sampling theorem in space.

The idea behind multiresolution parameter estimation is to obtain two or more estimates of  $\mu$ : the first based on a small baseline or short sampling period, yielding a coarse estimate  $\mu_1$  of  $\mu$  without aliasing, and the second based on a large baseline or (much) larger sampling period, providing an aliased estimate  $\mu_2$  of  $\mu$  at a finer scale. These two estimates are combined to obtain a final estimate  $\hat{\mu} = 2\pi n + \mu_2$ , where the integer number of cycles  $n$  is estimated from  $\mu_1$ . The ratio of the largest baseline to the shortest baseline (which is denoted by  $k_s$  and referred to as the *resolution gain factor*) is a measure of the gain in resolution. In this work, we find the bounds on  $k_s$  that will allow the proper functioning of the MR-ESPRIT algorithm.

Similar works have been reported in the literature. In particular, Zoltowski *et al.* [7] discuss a similar problem of angle-frequency estimation using multiple scales in time and space. Because of ambitious goals, however, their solutions are very much directed

Manuscript received April 14, 1998; revised December 28, 1998. This work was supported by TNO-FEL, The Hague, The Netherlands. The associate editor coordinating the review of this paper and approving it for publication was Prof. Victor A. N. Barosso.

The authors are with Department of Electrical Engineering, Delft University of Technology, Delft, The Netherlands (e-mail: aweke@cas.et.tudelft.nl).

Publisher Item Identifier S 1053-587X(99)03682-X.

by engineering considerations, which incurs a certain sacrifice in elegance and clarity. In particular, the coarse frequency estimation is done by applying ESPRIT to a small set of DFT values around spectral peaks that are determined via peak searching algorithms. The fine frequency estimates and the angle estimates are obtained sequentially and for each estimated coarse frequency independently, which assumes that they are sufficiently unique. Here, we derive a one-shot joint estimation procedure referred to as MR-ESPRIT.

There is a connection of MR-ESPRIT to MI-ESPRIT [8], [9] as well. MI-ESPRIT, like the MR-ESPRIT, exploits the multiple shift-invariance structure present in multibaseline arrays. A distinction is that MI-ESPRIT is formulated in terms of (iterative) subspace fitting and basically attempts to find more accurate beamforming vectors by considering multiple shift invariances. The original paper [8] did not specifically recognize the fact that also more accurate direction estimates can be found. In [9], a noniterative MI-ESPRIT is given. There, the aliasing is resolved by searching for an optimum solution among formerly computed candidates. Our approach, on the other hand, resolves aliasing by merely solving a set of analytic expressions. Moreover, the corresponding parameters are grouped automatically without the need for any extra processing, which is not the case in MI-ESPRIT.

## II. THE MR-ESPRIT

The original ESPRIT algorithm is based on arrays with a doublet structure, i.e., consisting of several antenna pairs with the same baseline vectors. The chosen array geometries often admit other pairings with different baselines. For instance, the array structure shown in Fig. 1 combines two spatial sampling rates. The minimal number of antennas to having two baseline vector pairs is four. With more antennas, several interesting configurations are possible.

The  $M$ -dimensional array response vector  $\mathbf{a}(\alpha)$  is defined as the response of the  $M$ -element antenna array to a narrowband signal from a direction  $\alpha$ . It can be parameterized in several ways. The usual parameterization is in terms of  $\theta = e^{j2\pi\Delta \sin(\alpha)}$ , where  $\Delta$  is a reference interantenna spacing smaller than half a wavelength. In our case of an array with two baselines, we can (redundantly) parameterize the array by two parameters  $\theta_1 = e^{j2\pi\Delta_1 \sin(\alpha)}$  and  $\theta_2 = e^{j2\pi\Delta_2 \sin(\alpha)}$ . In the case of the array of Fig. 1, we have

$$\mathbf{a}(\theta_1, \theta_2) = \begin{bmatrix} 1 \\ \theta_1 \\ \theta_2 \\ \theta_1\theta_2 \end{bmatrix}. \quad (1)$$

The idea is to treat the two parameters as independent and estimate both of them from the measured data and only then combine them into a single estimate of  $\sin(\alpha)$ . Estimation is done by exploiting the dual shift-invariance structure of  $\mathbf{a}(\theta_1, \theta_2)$ , i.e., in the above example

$$\begin{aligned} \mathbf{a}_{x1} &= \begin{bmatrix} a_1 \\ a_3 \end{bmatrix}, & \mathbf{a}_{y1} &= \begin{bmatrix} a_2 \\ a_4 \end{bmatrix} \Rightarrow \mathbf{a}_{y1} = \mathbf{a}_{x1}\theta_1 \\ \mathbf{a}_{x2} &= \begin{bmatrix} a_1 \\ a_2 \end{bmatrix}, & \mathbf{a}_{y2} &= \begin{bmatrix} a_3 \\ a_4 \end{bmatrix} \Rightarrow \mathbf{a}_{y2} = \mathbf{a}_{x2}\theta_2 \end{aligned}$$

where  $a_i$  is the  $i$ th entry of  $\mathbf{a}(\theta_1, \theta_2)$ . For more general arrays with a dual shift-invariance structure, we can define selection matrices  $\mathbf{J}_{x_i}$  and  $\mathbf{J}_{y_i}$  ( $i = 1, 2$ ) such that the above relations hold for  $\mathbf{J}_{x_i}\mathbf{a}$  and  $\mathbf{J}_{y_i}\mathbf{a}$ .

Let  $\mu_i$  ( $i = 1, 2$ ) be the argument of  $\theta_i$ . Then, if the distance  $\Delta_i < 1/2$ , the angle of arrival  $\alpha$  of the wavefront can be uniquely determined from  $\mu_i$  using the transformation

$$\alpha = \arcsin\left(\frac{\mu_i}{2\pi\Delta_i}\right).$$

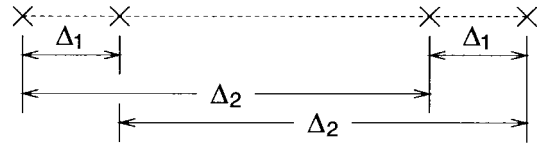


Fig. 1. Multiresolution spatial sampling.

However, when  $\Delta_i > 1/2$ , because of aliasing, we get a set of cyclically related candidates for  $\alpha$ :

$$\alpha(n) = \arcsin\left(\frac{\mu_i + 2\pi n}{2\pi\Delta_i}\right).$$

In MR-ESPRIT, we combine nonaliased and aliased estimates of the parameters to obtain a better estimation accuracy. The resulting algorithm is very similar to the case of joint azimuth-elevation estimation [10].

Thus, to be specific, consider  $d$  narrowband sources  $s_i(t)$  impinging on the antenna array. Collecting  $N$  output samples of the  $M$  antenna outputs into an  $M \times N$  data matrix  $\mathbf{X}$  in the usual way, we obtain the data model

$$\mathbf{X} = \mathbf{A}\mathbf{S} = \mathbf{a}_1\mathbf{s}_1 + \cdots + \mathbf{a}_d\mathbf{s}_d$$

where the columns of  $\mathbf{a}$  are the array response vectors  $\{\mathbf{a}_i\}$ , and the rows of  $\mathbf{S}$  are the sampled source signals. Assuming  $d < M$ , the first step of the algorithm is to estimate a basis  $\mathbf{U}_s$  of the column span of  $\mathbf{X}$ , typically using an SVD.  $\mathbf{U}_s$  and  $\mathbf{A}$  are related by a  $d \times d$  nonsingular matrix  $\mathbf{T}$  as

$$\mathbf{U}_s = \mathbf{A}\mathbf{T}.$$

The second step in the algorithm is to form submatrices of  $\mathbf{U}_s$  using the proper selection matrices

$$\mathbf{U}_{x_i} = \mathbf{J}_{x_i}\mathbf{U}_s, \quad \mathbf{U}_{y_i} = \mathbf{J}_{y_i}\mathbf{U}_s, \quad (i = 1, 2).$$

The shift-invariance structure of the array implies that

$$\mathbf{U}_{x_i} = \mathbf{A}'\mathbf{T}, \quad \mathbf{U}_{y_i} = \mathbf{A}'\Theta_i\mathbf{T}$$

where  $\mathbf{A}'$  is a submatrix of  $\mathbf{A}$ , and the diagonal matrix  $\Theta_i = \text{diag}\{\theta_{ij}\}_{j=1}^d$  contains the  $d$  shift parameters of the  $d$  sources with reference to the  $i$ th baseline. The final step is to estimate the parameters by considering

$$\begin{aligned} \mathbf{E}_1 &= \mathbf{U}_{x1}^\dagger \mathbf{U}_{y1} = \mathbf{T}^{-1} \Theta_1 \mathbf{T} \\ \mathbf{E}_2 &= \mathbf{U}_{x2}^\dagger \mathbf{U}_{y2} = \mathbf{T}^{-1} \Theta_2 \mathbf{T}. \end{aligned}$$

It is seen that the data matrices  $\mathbf{E}_1$  and  $\mathbf{E}_2$  are jointly diagonalizable by the same matrix  $\mathbf{T}$ . There are several algorithms to compute this joint diagonalization, e.g., by means of Jacobi iterations [10] or QZ iterations [11], [12]. For this to work, it is necessary that each submatrix  $\mathbf{U}_{x_i}$  has at least  $d$  rows. After  $\mathbf{T}$  has been found, we also have estimates of  $\{(\theta_{1j}, \theta_{2j})\}$  for each of the  $d$  sources.

It remains for each source to combine  $\theta_1$  and  $\theta_2$  into an estimate of the argument  $\mu$  of  $\theta$ . Let us assume that  $\Delta_1 \leq 1/2$  so that  $\mu_1$  (argument of  $\theta_1$ ) is not aliased and is a coarse estimate of  $\mu$ . In addition, assume that  $\Delta_2 \gg 1/2$  so that in  $\mu_2$ , aliasing occurs. The estimate  $\mu$  is proportional to  $\mu_2$  plus an appropriate integer multiple of  $2\pi$  (see Fig. 2). It follows that we have two estimates of  $2\pi \sin(\alpha)$

$$2\pi \sin(\alpha) = \frac{1}{\Delta_1} \mu_1 = \frac{1}{\Delta_2} (2\pi n + \mu_2). \quad (2)$$

The winding number  $n$  is determined as the best fitting integer to match the two right-hand side expressions

$$n = \text{round}\left(\frac{1}{2\pi} \left(\frac{\Delta_2}{\Delta_1} \mu_1 - \mu_2\right)\right) =: \text{round}(\hat{n}). \quad (3)$$

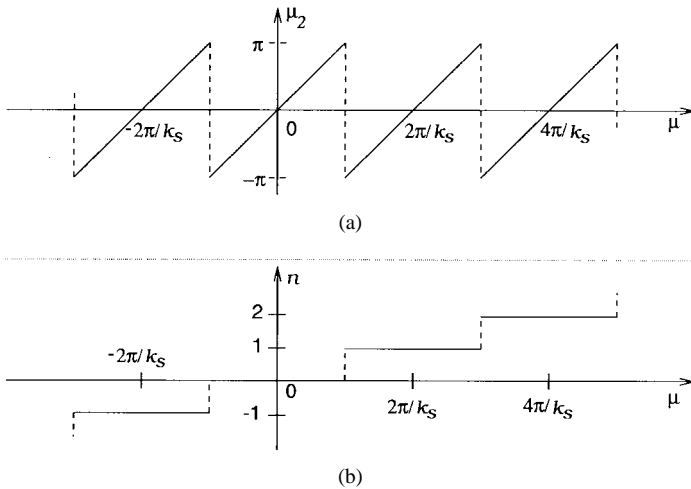


Fig. 2. (a) Aliased spatial frequency  $\mu_2$  as a function of the alias-free spatial frequency  $\mu$ . (b) Corresponding winding number  $n$ .

The ratio  $k_s := \Delta_2/\Delta_1$  can be interpreted as the (spatial) gain in resolution. In particular, the estimate of  $2\pi \sin(\alpha)$  based on  $\mu_2$  is a factor  $k_s$  more accurate than that based on  $\mu_1$ . Thus, a more accurate estimate of the spatial frequency  $\mu$  can be obtained as

$$\mu = \frac{1}{k_s}(2\pi n + \mu_2). \quad (4)$$

### III. ANALYSIS

#### A. The Winding Number

Consider the relations given in (3) and (4), where we have tacitly assumed that the relation  $\Delta_2 = k_s \Delta_1$  holds perfectly. In practice, however, due to measurement errors, this holds only approximately. Let  $\Delta k_s$  represent the error on  $k_s$  such that  $\Delta_2 = (k_s + \Delta k_s) \Delta_1$ . In addition, assume that  $\mu_1$  and  $\mu_2$  are determined with estimation errors  $\Delta\mu_1$  and  $\Delta\mu_2$ , respectively. We further assume that  $\Delta\mu_1$  and  $\Delta\mu_2$  are independent processes, with  $E\{\Delta\mu_1^2\} = E\{\Delta\mu_2^2\} = \sigma_\mu^2$ . With these assumptions, the error  $\Delta n$  on  $\hat{n}$  in (3) can be approximated as

$$\Delta n \approx \frac{\partial \hat{n}}{\partial k_s} \Delta k_s + \frac{\partial \hat{n}}{\partial \mu_1} \Delta \mu_1 + \frac{\partial \hat{n}}{\partial \mu_2} \Delta \mu_2.$$

Replacing the value of  $\hat{n}$  from (3) into the above equation, we obtain

$$\Delta n = \frac{1}{2\pi} \mu_1 \Delta k_s + \frac{1}{2\pi} (k_s \Delta \mu_1 - \Delta \mu_2). \quad (5)$$

For a given array configuration, the first term in (5) is a constant. It represents the offset in  $\hat{n}$  due to the array imperfection. On the other hand, both parameters  $\Delta\mu_1$  and  $\Delta\mu_2$  in the second term are zero mean Gaussian processes<sup>1</sup> [2]–[4]. Consequently,  $\Delta n$  is also a Gaussian process with a mean  $(1/2\pi)\mu_1 \Delta k_s$  and a variance

$$\sigma_n^2 = E\left\{\left(\Delta n - \frac{1}{2\pi} \mu_1 \Delta k_s\right)^2\right\} = \frac{1}{4\pi^2} (k_s^2 + 1) \sigma_\mu^2. \quad (6)$$

A typical distribution function of  $\Delta n$  is shown in Fig. 3. It is seen from (3) that  $n$  is determined correctly if  $|\Delta n| < 0.5$ . However, since  $\Delta n$  is a random process, we can satisfy this only with some uncertainty (confidence level). In particular, given a required confidence level  $\mathcal{L}$ , we find the conditions under which the probability

$$P(|\Delta n| < 0.5) > \mathcal{L}. \quad (7)$$

<sup>1</sup>More precisely, these are Gaussian processes if the input noise is Gaussian.

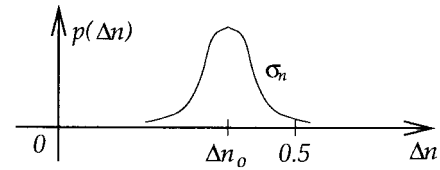


Fig. 3. Typical probability distribution function of  $\Delta n$ , [ $\Delta n_0 = (1/2\pi)\mu_1 \Delta k_s$ ].

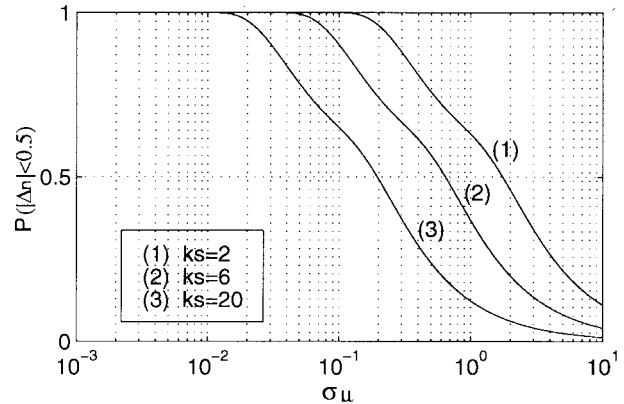


Fig. 4. Family of curves  $P(|\Delta n| < 0.5)$  as functions of  $\sigma_\mu$  for  $\mu_1 = \pi$  and  $\Delta k_s = 0.75$ .

Assuming that  $P(\cdot)$  is a Gaussian process, it can be shown [13] that

$$P(|\Delta n| < 0.5) = \frac{1}{2} \operatorname{erf}\left(\frac{\pi + \mu_1 \Delta k_s}{\sigma_\mu \sqrt{2(k_s^2 + 1)}}\right) + \frac{1}{2} \operatorname{erf}\left(\frac{\pi - \mu_1 \Delta k_s}{\sigma_\mu \sqrt{2(k_s^2 + 1)}}\right)$$

where  $\sigma_\mu$  represents the root mean square measurement error on  $\mu$ . A family of curves  $P(|\Delta n| < 0.5)$  for  $\mu_1 = \pi$  (representing worst-case scenario) and an arbitrarily chosen value of  $\Delta k_s = 0.75$  as functions of  $\sigma_\mu$  (for different values of  $k_s$ ) are shown in Fig. 4. To obtain more explicit expressions, let the function  $f(x)$  be defined as

$$f(x) = \frac{1}{2} [\operatorname{erf}(x(\pi + \mu_1 \Delta k_s)) + \operatorname{erf}(x(\pi - \mu_1 \Delta k_s))]. \quad (8)$$

Then,  $P(|\Delta n| < 0.5)$  may be expressed in terms of  $f(x)$  as

$$P(|\Delta n| < 0.5) = f\left(\frac{1}{\sigma_\mu \sqrt{2(k_s^2 + 1)}}\right).$$

Now, putting this into (7) and solving for  $k_s$ , we get

$$k_s < \sqrt{\frac{1}{2\sigma_\mu^2} \left(\frac{1}{f^{-1}(\mathcal{L})}\right)^2 - 1} =: k_{\max} \quad (9)$$

where  $f^{-1}(\cdot)$  is the inverse function of  $f(\cdot)$ . From this relation, it is clear that the resolution gain factor cannot be made arbitrarily large. It is bounded from above by a number that is a function of the estimation error and the array imperfection factor  $\Delta k_s$ . Particularly, we can clearly see that as the estimation error increases, the maximum value of  $k_s$  decreases. This is in perfect agreement with intuitive perception. For instance, for the case  $\mu_1 = \pi$ ,  $\Delta k_s = 0.75$ , and  $\mathcal{L} = 0.998$ , the bounds on  $k_s$  at  $\sigma_\mu = 0.1$  and  $0.05$  are 9 and 17.6, respectively.

#### B. Dependence of $k_{\max}$ on SNR

To establish the relation between  $k_s$  and SNR, we first need to determine the dependence of  $\sigma_\mu$  (the phase estimation error) on the

SNR. To this end, in [5] and [6], it is shown that the DOA estimation error and the SNR are related as

$$\sigma_{\alpha_i}^2 = \frac{1}{\text{SNR}} \left( \frac{1}{M^2 N} \left( \frac{1}{2\pi\Delta_i \cos(\alpha)} \right)^2 \right) \quad (10)$$

where  $\sigma_{\alpha_i}$  is the root mean square error (RMSE) obtained with reference to the  $i$ th base line separation  $\Delta_i$ . Recall that  $\mu_i = 2\pi\Delta_i \sin(\alpha)$  and, hence

$$\begin{aligned} \mu_i + \Delta\mu_i &= 2\pi\Delta_i \sin(\alpha + \Delta\alpha) \\ &\approx 2\pi\Delta_i (\sin(\alpha) + \Delta\alpha \cos(\alpha)). \end{aligned}$$

This implies that  $\Delta\mu_i = (2\pi\Delta_i \cos(\alpha))\Delta\alpha$  and

$$\sigma_{\mu}^2 = (2\pi\Delta_i \cos(\alpha))^2 \sigma_{\alpha_i}^2 \quad (11)$$

Here, the index reference to the baseline in  $\sigma_{\mu}^2 = E\{(\Delta\mu_i)^2\}$  is dropped because  $\Delta\mu_i$  is independent of  $\Delta_i$ . Now, using (10),  $\sigma_{\mu}^2$  is expressed in terms of array parameters as

$$\sigma_{\mu}^2 = \frac{1}{\text{SNR}} \left( \frac{1}{M^2 N} \right) \quad (12)$$

Finally, putting (12) into (9), we find the following expression for  $k_{\max}$ :

$$k_{\max} = \sqrt{\frac{\text{SNR}}{2} \left( M^2 N \left( \frac{1}{f^{-1}(\mathcal{L})} \right)^2 \right) - 1}. \quad (13)$$

Note that (10) and, therefore, (13) are derived, assuming that there is only one source in the channel. For more than one source ( $d$  sources, say), let  $\sigma_{\mu_j}$  represent the variance of the phase estimation error of the  $j$ th source.<sup>2</sup> Then, the bound on  $k_s$  is generalized as

$$k_{\max} = \min_{j=1 \dots d} \sqrt{\frac{1}{2\sigma_{\mu_j}^2} \left( \frac{1}{f_j^{-1}(\mathcal{L})} \right)^2 - 1}$$

where  $f_j(\cdot)$  is as defined in (8), but with  $\mu_1$  replaced by  $\mu_{1j}$  (the  $j$ th phase shift measured with reference to  $\Delta_1$ ).

### C. Bias on $\mu$ Due to Imperfect Array and a Self-Calibrating MR-ESPRIT

Once the winding number  $n$  is determined correctly, the next step is to use (4) to estimate the spatial frequency  $\mu$ . If the array is imperfect, the estimate of  $\mu$  will be biased. The bias (offset)  $\Delta\mu$  on  $\mu$  due to  $\Delta k_s$  can be approximated by (viz. 4)

$$\Delta\mu \approx \frac{\partial\mu}{\partial k_s} \Delta k_s = \frac{1}{k_s^2} (2\pi n + \mu_2) \Delta k_s \quad (14)$$

which indicates that for a given value of  $k_s$ , angles associated with large winding numbers are more affected by  $\Delta k_s$  than those associated with small winding numbers. To minimize this bias, a *self-calibrating MR-ESPRIT* may be implemented as described in [14].

## IV. SIMULATION

In this section, we give simulation results that confirm our theory. The simulation example considers a processing band of 10 MHz and a linear antenna array with  $M = 4$  antenna elements arranged as in Fig. 1 with  $\Delta_1 = 1/2$  and varying  $\Delta_2$ . The data is collected into a  $4 \times 64$  matrix at a sampling rate of  $F_1 = 20$  MHz. Two sources emitting narrowband signals (25 kHz) at center frequencies  $f = [6, 6.5]$  MHz, and propagating in distinct directions with DOA's  $\alpha = [40, 45]^\circ$  are considered.

<sup>2</sup>For more than one source,  $\sigma_{\mu}$  depends on the SNR in a more complicated way. Refer to [4] and [6] for more information.

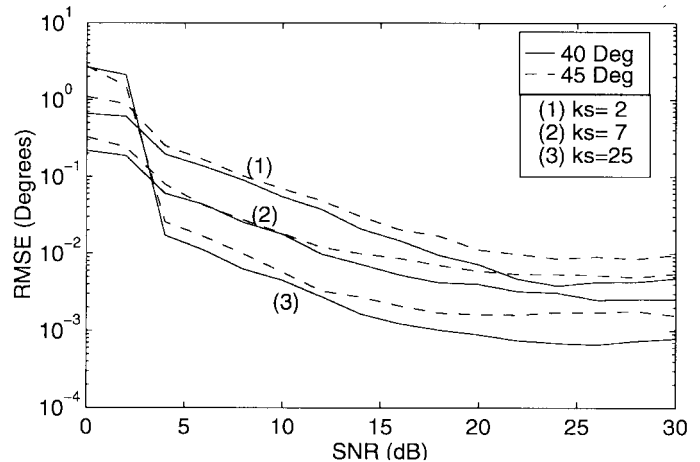


Fig. 5. Root mean square error of the frequency estimates as functions of SNR. ( $k_s = 2$  corresponds to ULA).

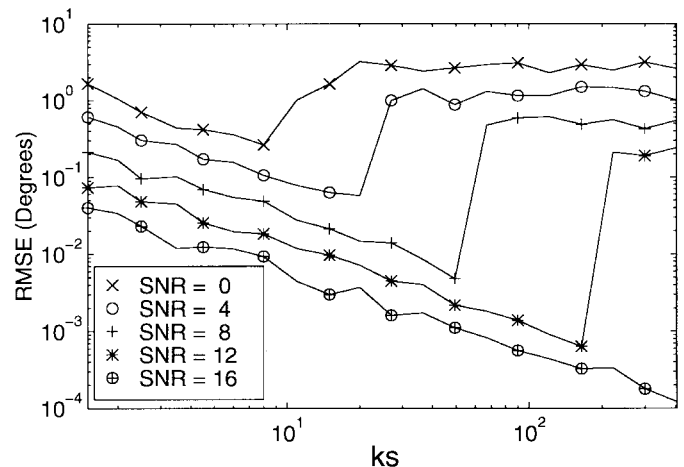


Fig. 6. Root mean square error of the DOA estimates, corresponding to the wavefront with DOA =  $45^\circ$  as functions of  $k_s$ .

The results are shown in Figs. 5 and 6. From the first plot, it is seen that the accuracy of MR-ESPRIT is proportional to the gain factor  $k_s$ . An upper limit for this gain is reached when the winding numbers  $n$  can no longer be estimated accurately. This is shown in Fig. 6, where the RMSE of the parameter estimator as a function of varying  $k_s$  is analyzed. To make the figure less crowded, only the behavior corresponding to DOA =  $45^\circ$  is plotted. It is seen that for given SNR, there exists a limit on  $k_s$  beyond which the performance of the estimator degrades sharply. Moreover, this bound is seen to be proportional to the SNR, as expected.

## REFERENCES

- [1] R. H. Roy, "ESPRIT-estimation of signal parameters via rotational invariance techniques," Ph.D. dissertation, Stanford Univ., Stanford, CA, 1987.
- [2] M. Viberg, B. Ottersten, and A. Nehorai, "Performance analysis of direction finding with large arrays and finite data," *IEEE Trans. Signal Processing*, vol. 43, pp. 469–477, Feb. 1995.
- [3] M. Viberg and B. Ottersten, "Sensor array processing based on subspace fitting," *IEEE Trans. Signal Processing*, vol. 39, pp. 1110–1121, May 1991.
- [4] B. Ottersten, M. Viberg, and T. Kailath, "Performance analysis of the total least squares ESPRIT algorithm," *IEEE Trans. Signal Processing*, vol. 39, pp. 1122–1135, May 1991.

- [5] B. D. Rao and K. V. S. Hari, "Performance analysis of root-music," *IEEE Trans. Acoust., Speech, Signal Processing*, vol. 37, pp. 1939–1949, Dec. 1989.
- [6] —, "Performance analysis of ESPRIT and TAM in determining the direction of arrival of plane waves in noise," *IEEE Trans. Acoust., Speech, Signal Processing*, vol. 37, pp. 1990–1995, Dec. 1989.
- [7] M. D. Zoltowski and C. P. Mathews, "Real-time frequency and 2-D angle estimation with sub-Nyquist spatio-temporal sampling," *IEEE Trans. Signal Processing*, vol. 42, pp. 2781–2794, Oct. 1994.
- [8] A. Lee Swindlehurst, B. Ottersten, R. Roy, and T. Kailath, "Multiple invariance ESPRIT," *IEEE Trans. Signal Processing*, vol. 40, pp. 867–881, Apr. 1992.
- [9] K. T. Wong and M. D. Zoltowski, "Closed-form multi-dimensional multi-invariance ESPRIT," in *Proc. ICASSP*, Munich, Germany, Apr. 1997, pp. 3489–3493.
- [10] A.-J. van der Veen, P. B. Ober, and E. F. Deprettere, "Azimuth and elevation computation in high resolution DOA estimation," *IEEE Trans. Signal Processing*, vol. 40, pp. 1828–1832, July 1992.
- [11] A.-J. van der Veen and A. Paulraj, "An analytical constant modulus algorithm," *IEEE Trans. Signal Processing*, vol. 44, pp. 1136–1155, May 1996.
- [12] L. de Lathauwer, "Signal processing based on multilinear algebra," Ph.D. dissertation, Katholieke Univ. Leuven, Leuven, Belgium, 1997.
- [13] S. Haykin, *An Introduction to Analog and Digital Communications*. New York: Wiley, 1986.
- [14] A. N. Lemma, A.-J. van der Veen, and E. F. Deprettere, "On the multi-resolution ESPRIT algorithm," in *Proc. Ninth SP Workshop SSAP*, Portland, OR, Sept. 1998.

## Analysis of Spatial Smoothing with Uniform Circular Arrays

K. Maheswara Reddy and V. U. Reddy

**Abstract**—In this correspondence, we analyze spatial smoothing with uniform circular arrays (UCA's). In particular, we study the performance of the Root-MUSIC with smoothing in the presence of correlated sources, finite data perturbations, and errors in transformed steering vector that arise due to some approximations made while extending the Root-MUSIC and smoothing to UCA. Expressions are derived for the asymptotic performance of the Root-MUSIC with smoothing applied to the transformed UCA data. An attempt has been made to bring out the impact of both the forward and forward-backward smoothing. We consider UCA's with isotropic as well as directional sensors in our study. Computer simulations are provided to demonstrate the usefulness of the analysis.

### I. INTRODUCTION

Uniform circular arrays (UCA's) are commonly employed when 360° coverage is required in the plane of the array. Circular arrays are nonuniform linear arrays, and hence, the rooting techniques and preprocessing schemes like spatial smoothing [7] cannot be directly applied to these arrays. In [8], Tewfik and Hong have shown that it is possible to extend the Root-MUSIC to UCA using the phase mode excitation concept. In [2], Mathews and Zoltowski proposed

Manuscript received December 11, 1996; revised November 19, 1998. The associate editor coordinating the review of this paper and approving it for publication was Dr. Gary F. Hatke.

K. M. Reddy is with CASSA, Defence Research and Development Organization, New Thippasandra, Bangalore, India.

V. U. Reddy is with the Department of Electrical Communication Engineering, Indian Institute of Science, Bangalore, India.

Publisher Item Identifier S 1053-587X(99)03679-X.

real beamspace MUSIC to UCA that yields reduced computation and better resolution. In [10] and [11], the authors extend spatial smoothing to UCA's.

While extending the rooting techniques to UCA, all the authors assumed that some of the terms in the transformed steering vector of UCA are negligible when the circumferential spacing between the elements is less than half wavelength. These approximations cause errors in the DOA estimates obtained with the Root-MUSIC, even when the number of snapshots tends to infinity, and we analyze the effect of smoothing on these errors in this correspondence. We also extend smoothing to UCA's with directional elements.

### II. BACKGROUND

Consider a UCA with  $L$  identical and omnidirectional sensors. Let  $r$  be the radius of the array and  $d$  be the circumferential spacing between the elements. Let  $\theta$  denote the angle (azimuth angle) measured in the plane containing the elements. We assume for simplicity that the sources are in the same plane as the UCA. The steering vector of the UCA w.r.t. the center of the array can then be expressed as

$$\mathbf{a}_c(\theta) = [e^{j\xi \cos \theta}, e^{j\xi \cos(\theta-2\pi/L)}, \dots, e^{j\xi \cos(\theta-2\pi(L-1)/L)}]^T \quad (1)$$

where  $\xi = 2\pi r/\lambda$ ,  $\lambda$  is the wavelength, and  $(\cdot)^T$  represents the transpose of  $(\cdot)$ . The weight vector that excites the array with  $m$ th phase mode is given by [2]  $\mathbf{w}_m^H = j^{-|m|}/L [1, e^{j2\pi m/L}, \dots, e^{j2\pi m(L-1)/L}]$ . The array pattern for the  $m$ th phase mode is [1], [2]

$$f_m(\theta) = \mathbf{w}_m^H \mathbf{a}_c(\theta) = J_{|m|}(\xi) e^{jm\theta} + j^{-|m|} \sum_{q=1}^{\infty} [j^q J_q(\xi) e^{-jq\theta} + j^h J_h(\xi) e^{jh\theta}] - \mathcal{D} \leq m \leq \mathcal{D} \quad (2)$$

where  $\mathcal{D}$  is the maximum number of phase modes and given by [2]  $\mathcal{D} \simeq [2\pi r/\lambda]$ ,  $J_m(\xi)$  is the Bessel function of the first kind of order  $m$ ,  $h = Lq + m$ ,  $g = Lq - m$ ,  $(\cdot)^H$  represents the complex conjugate transpose of  $(\cdot)$ , and  $[x]$  denotes the largest integer less than or equal to  $x$ . The first term in (2) becomes dominant if  $d$  is less than  $0.5\lambda$ . In our analysis, we consider  $d < 0.5\lambda$  and assume the second term of (2) to be small.

The normalized transformation matrix  $\mathbf{F}$  to excite the array patterns corresponding to  $(2\mathcal{D} + 1)$  phase modes is given by  $\mathbf{F} = \sqrt{L}[\mathbf{w}_{-\mathcal{D}}, \dots, \mathbf{w}_0, \dots, \mathbf{w}_{\mathcal{D}}]$ . Using this transformation, we express

$$\mathbf{a}_t(\theta) = \mathbf{F}^H \mathbf{a}_c(\theta) = \mathbf{J}_\xi \mathbf{a}(\theta) + \Delta \mathbf{a}(\theta) \quad (3)$$

where  $\mathbf{J}_\xi = \sqrt{L} \text{diag}[J_{\mathcal{D}}(\xi), \dots, J_1(\xi), J_0(\xi), J_1(\xi), \dots, J_{\mathcal{D}}(\xi)]$

$$\mathbf{a}(\theta) = [e^{-j\mathcal{D}\theta}, e^{-j(\mathcal{D}-1)\theta}, \dots, 1, \dots, e^{j(\mathcal{D}-1)\theta}, e^{j\mathcal{D}\theta}]^T \quad (4)$$

and  $\Delta \mathbf{a}(\theta)$  is the contribution due to the second term in (2). Note that the vector  $\mathbf{a}(\theta)$  has a structure similar to that of the steering vector of a uniform linear array (ULA). We treat  $\Delta \mathbf{a}(\theta)$  as the error in the transformed steering vector caused due to approximation.

Assume that  $M$  sources are impinging on the UCA and the DOA's of these sources are  $\theta_1, \theta_2, \dots, \theta_M$ . The covariance matrix at the output of UCA can be expressed as

$$\mathbf{R}_c = \mathbf{A}_c \mathbf{S} \mathbf{A}_c^H + \sigma^2 \mathbf{I} \quad (5)$$